



Cloudy sky contributions to the direct aerosol effect

Gunnar Myhre¹, Bjørn H. Samset¹, Christian W. Mohr¹, Kari Alterskjær¹, Yves Balkanski², Nicholas Bellouin³, Mian Chin⁴, James Haywood^{5,6}, Øivind Hodnebrog¹, Stefan Kinne⁷, Guangxing Lin^{8,9}, Marianne T. Lund¹, Joyce. E. Penner¹⁰, Michael Schulz¹¹, Nick Schutgens¹², Ragnhild B. Skeie¹, Philip Stier¹³, Toshihiko Takemura¹⁴, Kai Zhang¹⁵

¹CICERO Center for International Climate Research, Oslo, Norway.

²Laboratoire des Sciences du Climat et de l'Environnement, CEA-CNRS-UVSQ-UPSaclay, Gif-sur-Yvette, France.

³Department of Meteorology, University of Reading, Reading, RG6 6BB, UK.

⁴NASA Goddard Space Flight Center, Greenbelt, MD 20771 USA.

10 ⁵College of Engineering, Mathematics and Physical Sciences, University of Exeter, Exeter, EX4 4QF, UK

⁶Earth System and Mitigation Science, Met Office Hadley Centre, Exeter, EX1 3PB, UK

⁷Max Planck Institute for Meteorology, Hamburg, Germany.

⁸University of Michigan, Ann Arbor, MI, USA.

⁹now at Atmospheric Sciences and Global Change Division, Pacific Northwest National Laboratory, Richland, WA, USA

15 ¹⁰Department of Climate and Space Sciences and Engineering, University of Michigan, U. S. A

¹¹Norwegian Meteorological Institute, Oslo, Norway.

¹²Earth Sciences, Faculty of Science, Vrije Universiteit Amsterdam, Amsterdam, Netherlands.

¹³Atmospheric, Oceanic and Planetary Physics, Department of Physics, University of Oxford, UK

¹⁴Research Institute for Applied Mechanics, Kyushu University, Fukuoka, Japan.

20 ¹⁵Pacific Northwest National Laboratory, Richland, WA, USA

Corresponding author: Gunnar Myhre (gunnar.myhre@cicero.oslo.no)

Abstract: The radiative forcing of the aerosol-radiation interaction can be decomposed into clear sky and cloudy sky portions. Two sets of multi-model simulations within AeroCom, combined with observational methods, and the time evolution of aerosol emissions over the industrial era show that the contribution from cloudy sky regions is likely weak. A mean of the simulations considered is $0.01 \pm 0.1 \text{ Wm}^{-2}$. Multivariate data analysis of results from AeroCom Phase II shows that many factors influence the strength of the cloudy sky contribution to the forcing of the aerosol-radiation interaction. Overall, single scattering albedo of anthropogenic aerosols and the interaction of aerosols with the shortwave cloud radiative effects are found to be important factors. A more dedicated focus on the contribution from the cloud free and cloud covered sky fraction respectively to the aerosol-radiation interaction will benefit the quantification of the radiative forcing and its uncertainty range.



1 Introduction

35 The radiative forcing (RF) of atmospheric aerosols due to the aerosol-radiation interaction – RFari (earlier denoted as direct aerosol effect) was assessed as -0.35 [-0.85 to $+0.15$] Wm^{-2} in the Fifth Assessment Report by the Intergovernmental Panel on Climate Change (IPCC) (AR5) (Boucher et al., 2013). The AR5 uncertainty range is even slightly wider than in the Fourth Assessment Report (Forster et al., 2007). Despite major progress in the understanding of atmospheric aerosol composition, and almost two decades of multi-aerosol type model simulations, little progress had been made in reducing the large uncertainty
40 in this number, until recently where Bellouin et al. estimate a range of -0.45 to -0.05 Wm^{-2} . Bellouin et al. estimate RFari from normalized clear sky radiative effect by aerosol optical depth (AOD) and multiply this by an assessment of anthropogenic AOD. No direct simulations were used to calculate the RFari in regions of clouds.

One reason for the larger uncertainty range in AR5 compared to AR4 was enhanced uncertainty and magnitude of the RFari of black carbon (BC) (Boucher et al., 2013). Bond et al. (2013) indicated that emission of BC was too low in the inventories applied in climate models and therefore scaled the RFari from models to observed Aeronet absorption aerosol optical depth (AAOD) retrievals. More recently it has been suggested that AAOD data from Aeronet may have a sampling bias due to sites being located close to emission source regions (Wang et al., 2018), but uncertain in magnitude (Schutgens, 2019) and that most global aerosol models may have a bias towards too much BC in the middle and upper troposphere (Kipling et al., 2013; Samset et al., 2014; Wang et al., 2014). Both of these factors indicate a too strong BC RFari in Bond et al. (2013). However,
45 the most recent fossil and biofuel BC emission inventory (Hoesly et al., 2018) is much higher than used in previous global modelling (Lamarque et al., 2010). These new findings indicate that the BC RFari may be stronger than what was given in some of the multi-model global aerosol modelling exercises (Myhre et al., 2013a; Schulz et al., 2006), but likely weaker than estimated in Bond et al. (2013). The uncertainties in the RFari are also large for other aerosol species. For nitrate (Bian et al., 2017) the abundance is particularly uncertain, and for organic aerosols uncertainties are large both due to abundance (Tsigaridis et al., 2014) and the optical properties, particularly for brown carbon (Samset et al., 2018).
50

A further complication when estimating RFari is the atmospheric mix of scattering and absorbing aerosols. Since RFari is dependent on aerosol optical properties and the underlying albedo (Haywood and Shine, 1997), it is therefore also very dependent on where the aerosols are located relative to clouds (Takemura et al., 2002). Absorbing aerosols above clouds have a strong positive RFari (Chand et al., 2009; Keil and Haywood, 2003) but it becomes considerably weaker if the aerosols are
60 located below clouds (Takemura et al., 2002). Scattering aerosols above or below clouds may enhance the reflection of solar radiation in conditions of thin clouds. The all sky RFari can be separated into contributions from clear and cloudy sky portions:

$$\mathbf{RFari}_{\text{all sky}} = (1 - \mathbf{AC}) * \mathbf{RFari}_{\text{clear}} + \mathbf{AC} * \mathbf{RFari}_{\text{cloud}} \quad (1)$$

AC is the cloud fraction, $\mathbf{RFari}_{\text{clear}}$ and $\mathbf{RFari}_{\text{cloud}}$ are the clear sky and cloudy sky RFari, respectively. All three variables vary as a function of longitude, latitude and time. The RFari is the initial perturbation to top of the atmosphere (TOA) radiative fluxes (the instantaneous RF which for aerosol is very similar to RF). Rapid adjustments from absorption by aerosols mostly
65



BC, may alter atmospheric temperatures, water vapour and clouds. The sum of RFari and rapid adjustments is denoted effective radiative forcing (Boucher et al., 2013; Myhre et al., 2013b; Sherwood et al., 2015). The rapid adjustment of absorbing aerosols can be strong and may counteract the RFari substantial (Smith et al., 2018). Since RFari includes no rapid adjustments, AC is constant in Equation 1. Oikawa et al. (2013); Oikawa et al. (2018) provide estimates of all sky, clear sky and cloudy sky radiative effect of aerosols in different regions based on satellite retrievals of clouds and aerosols. These studies further describe large differences resulting from whether aerosols are below or above clouds. Lacagnina et al. (2017); Zhang et al. (2016) found large regional variation in the radiative effect of aerosols above clouds. Note that the above-mentioned studies investigate the current, total aerosol abundance which consist of anthropogenic and natural aerosols, whereas in terms of RFari only the anthropogenic aerosols are considered. Matus et al. (2019) combined satellite derived aerosol radiative effect with model simulation of anthropogenic aerosol, to make an estimate of RFari.

The aim of the present study is to provide insight into factors determining the contribution from cloudy sky regions to the RFari (second term on the right-hand side of equation 1) from combining global models and observations. We present estimates of this quantity from several global studies and we use multivariate data analysis to provide insight on the core factors causing the diversity among models.

80 2 Methods

2.1 Global estimates of cloudy sky contribution to RFari

The models, experiments and RFari from AeroCom Phase I and II are documented in detail by Schulz et al. (2006) and Myhre et al. (2013a), respectively. We also analyze the historical evolution of RFari due to anthropogenic aerosols using output from a series of OsloCTM3 simulations (Lund et al., 2018) with emissions from the Community Emission Data System (CEDS) (Hoesly et al., 2018) inventory from year 1750 to 2014. The OsloCTM3 is a global 3-dimensional chemistry-transport model driven by 3-hourly meteorological forecast data.

The analysis is further supplemented by variables from Equation 1 extracted from Myhre (2009), who presented results from OsloCTM2 and an observational based method to explain the difference in all sky RFari between observational based and global aerosol model approaches. The model simulations were made to investigate several assumptions on aerosol optical properties and impacts of assumptions related to missing data and change in industrial era aerosol concentration for the observational method. The Max Planck Aerosol Climatology version 2 (MACv2) method combines aerosol optical properties from Aeronet, surface albedo and clouds from ISCCP, vertical profiles of absorbing aerosols from the ECHAM-HAM model, with multi-model mean data on anthropogenic fraction from AeroCom Phase I (Kinne, 2019a; Kinne, 2019b).

The cloudy sky contribution to all sky RFari is calculated from daily or monthly diagnostics of allsky RFari, RFari_{clear} and AC. RF is taken at the top of the atmosphere and all estimates are from pre-industrial to present.



2.2 Multivariate data analysis

Multivariate data analysis in this study is based on results from a subset of the models participating in AeroCom Phase II (CAM5, GOCART, HadGEM2, IMPACT, INCA, ECHAM-HAM, OsloCTM2 and SPRINTARS). These eight models participated in AeroCom Phase II experiment (Myhre et al., 2013a) with no constrain on aerosol processes and in addition the host model AeroCom exercise with fixed aerosol optical properties (Stier et al., 2013). From the latter FIX2 and FIX3 experiments can be used to retrieve the contributions from cloudy sky to RFari in two highly idealized aerosol radiative properties experiments. FIX2 is a purely scattering aerosol case and FIX3 is an absorbing aerosol case. The origin of the different variables derived from AeroCom phase II model simulations (Myhre et al., 2013a; Samset et al., 2013) can be found Table 1.

The data is analyzed using principal component analysis (PCA). Here, the variables that may influence the cloudy sky RFari contribution to all sky RFari are orthogonally transformed into linearly uncorrelated variables named principal components (PCs). The transformation is defined so that the first principal component (PC1) accounts for most of variance exhibited by the underlying variables. Each following PC in turn has the highest variance possible assuming that it is orthogonal to the previous PC, successively explaining less of the magnitude of cloudy sky RFari. Data is normalized prior to PCA to ensure comparison of variance between variables. PCA results are usually plotted in a biplot, where only PC1 and PC2 (the second PC) are plotted on the x- and y-axis, respectively, since the two PCs explain most of the variance. In the biplot variables are projected as vectors along PC1 and PC2. The combined length and direction of the vector indicates the correlation the variable has with PC1 and PC2. Values range from -1 to 1 indicating negative to positive correlation with the PC. A value of 0 indicates no correlation with the PC. Since the projected vectors are directional it is possible to have high correlation with PC1 (values ~ -1 or ~ 1), and poor correlation with PC2 (value ~ 0), or *visa-versa*. Variables that point in the same direction are positively correlated with each other. Variables that point in the opposite direction of each other are negatively correlated. Variables that are perpendicular to each other are not correlated with each other or may be partially positively and partially negatively correlated. The missing data (see Table 1) for two of the models (LMDZ-INCA and ECHAM-HAM) are filled-in using regularized iterative PCA. This technique estimates the missing values, based on the correlation between the variables and the principal components (Josse and Husson, 2012).

The contribution of cloudy sky to RFari (“Cloudy”) (second term in Equation 1) is added as a supplementary variable in the PCA. This is to ensure that this dependent variable, the cloudy sky contribution, does not influence the projected correlations the independent variables have on each other. The same approach is applied to FIX2 and FIX3, as these variables are not independent, as they are composed of the many of the variables used in the analysis. In addition, linear regression correlation coefficients are calculated between all the variables to assess the individual relationships. No data imputation is used for the one to one linear regression.



3 Results

3.1 Estimates of cloudy sky contributions to RFari

Figure 1 shows the all sky RFari due to anthropogenic aerosols separated into clear sky (first term on right-hand side in equation 1) and cloudy sky (second term on right-hand side in equation 1) portion from AeroCom Phase II models (Myhre et al., 2013a). The uncertainty ranges given in the figure are one standard deviation among the global aerosol models in AeroCom Phase II. The figure shows two main results, that the cloudy sky RFari is weak and that the uncertainties in the contributions from cloudy sky and clear sky are substantial with the latter somewhat larger in magnitude.

Figure 2 shows an example from OsloCTM3 (Lund et al., 2018) of the spatial distribution of various terms given in equation 1. In the lower row of Figure 2 the annual mean AC, RFari_{clear} and RFari_{cloud} are shown, with strong negative RFari_{clear} over most land areas except over regions of high surface albedo such as deserts. The RFari_{cloud} is particularly positive over regions of biomass burning aerosols overlying low level stratocumulus, but also over parts of high aerosol abundance over China. The second row shows the two terms on the right hand in equation 1, namely the contribution from the cloud free and cloudy regions to the all sky RFari. The contribution from the clear sky regions (first term on the right-hand side of equation 1) is much weaker than RFari_{clear} itself since cloud fraction is high in many of the regions of anthropogenic aerosols. While the influence from cloud fraction on the cloudy sky contribution to all sky RFari relative to RFari_{cloud} is weak over biomass burning regions, it weakens relative to the negative values in RFari_{cloud} over many areas in the northern hemisphere. In the top row the RFari all sky is the sum of the contributions from clear and cloudy regions where their importance for the RFari varies regionally.

Figure 3a-d shows estimates of the contribution from cloud sky to RFari from several studies: two are multi-model studies, one combines model and observational based methods and one study investigates the time evolution using one model. The two multi-model AeroCom studies (Myhre et al., 2013a; Schulz et al., 2006) show that the sign varies among the global aerosol models and that two versions from one model changes sign between the two AeroCom phases (two versions of ECHAM-HAM, UIOCTM versus OsloCTM2, and UMI versus IMPACT). The two model versions INCA and LSCE have positive values in both AeroCom phases. SPRINTARS has the strongest positive (and overall strongest magnitude) of cloudy sky RFari contribution to all sky RFari in both AeroCom phases. About half of the models shown in Figure 3a and 3b have provided sufficient diagnostics to extract estimates from both AeroCom phases. The AeroCom PhaseII results will be further discussed in section 3.2.

In Myhre (2009) several experiments were performed to explain that differences in RFari between observational based methods and global aerosol models arise from a relatively larger change in absorbing aerosols over the industrial era than in the current abundance of the absorbing aerosols. Whereas an observational method uses aerosol optical properties from measurements of the present time of the combined natural and anthropogenic aerosols, the models simulate a relatively larger change in the abundance of anthropogenic absorbing aerosols than assuming no change in the industrial era aerosol optical properties. Figure



3c shows the contribution of the cloudy sky to RFari from several of these experiments. The two experiments
160 MODIS(SCREEN) and MODIS use satellite retrievals of aerosol optical depth (AOD), current aerosol optical properties
retrieved (single scattering albedo and asymmetry factor) from AERONET, and a model estimate of the anthropogenic AOD.
The difference between these experiments is that the MODIS experiment uses model information over regions of missing
AOD from the satellite retrievals, while these regions are ignored in MODIS(SCREEN). The contribution of cloudy sky to all
sky RFari is similar in these two experiments. On the other hand, in the experiment MODIS(Model), changes in the aerosol
165 optical properties from pre-industrial to present causes the change in sign in the cloud sky contribution to RFari compared to
MODIS and MODIS(SCREEN). The MODIS(Model) has very similar RFari, as well as cloudy sky contribution to all sky
RFari, to the standard global aerosol model simulations (MODEL INT and MODEL EXT). The two latter model simulations
differ on whether internal or external mixing of BC is taken into account or not, respectively. The MACv2 cloudy sky
contribution to RFari is -0.13 Wm^{-2} . This estimate does not consider change in the aerosol optical properties over the industrial
170 era and can thus be compared to MODIS(SCREEN) and MODIS experiments described above.

The time evolution of the contribution of cloudy sky to RFari in OsloCTM3 is shown in Figure 3d where all variations are
caused by changes in the anthropogenic aerosol composition and abundance since all other factors are kept constant. Values
are negative in the period 1960 to 1990 due to a strong increase in SO_2 emissions and thereby a domination of scattering
aerosols and radiative impacts even in cloudy skies. In the period after 1990 the regional SO_2 emissions have changed strongly,
175 but with a small reduction in the global emissions. Emissions of BC have on the other hand increased substantially making
anthropogenic aerosols more absorbing in the OsloCTM3 causing a relatively stronger positive contribution from the cloudy
sky to RFari.

3.2 Multivariate data analysis of cloudy sky contribution to the all sky RFari

Table 1 lists the AeroCom Phase II models and variables included in the multivariate data analysis for investigating
180 contributions to cloudy sky RF denoted as “Cloudy” in the table (the second term on the right-hand side of equation 1). The
results of the multivariate data analysis are plotted in a biplot and a correlogram Figure 4. The principal component analysis
(PCA) found that 68.2% of the total variance is explained by the first and second principal component (PC1 and PC2), see
Figure 4a. The analysis shows that several factors are important for the contribution of cloudy sky to RFari (“Cloudy”). Among
all variables total short-wave cloud radiative effect (SW_CRF) is the most important. Single scattering albedo (SSA) being a
185 crucial variable for the anthropogenic aerosols may potentially be an important factor (a higher SSA is expected to give a more
negative cloudy sky forcing). However, independent correlations plotted in the correlogram (Figure 4b) suggests that the
cloudy sky contribution to RFari and SSA is weak ($r = 0.17$). In depth analysis of the linear correlation between cloudy sky to
RFari and SSA suggests that the linear relationship exist only at higher PCs (see supplementary Figure S1).



The contribution of cloudy sky to RFari shows a closer dependence on similar quantities for the idealized experiment FIX3
190 than FIX2, where FIX2 has purely scattering aerosols. Both FIX2 and FIX3 are dependent on host model properties such as
clouds, surface albedo and radiative transfer schemes (Stier et al., 2013).

PCA finds negative correlation between cloudy sky contribution to RFari and total short-wave cloud radiative flux (SW_CRF),
also supported by the linear regression. One example here is the GOCART model with the weakest SW_CRF and most negative
cloudy sky contribution to RFari of the model included in the multivariate data analysis. At the same time the PCA finds small
195 dependence between the cloudy sky contribution to RFari and cloud fraction (CLD_FR) or cloud altitude (CL_ALT). The
negative correlation between cloudy sky contribution to RFari and SW_CRF can be explained by reflective clouds enhancing
the underlying albedo and thus making the radiative forcing more positive with an increase in absorbing aerosols in the cloudy
sky portion.

Overall FIX3 (where models have a fixed SSA) and SW_CRF seem to be the main explanatory variables for the variance in
200 the cloudy sky contribution to RFari. It is however worth noting that the correlation for cloudy sky contribution to RFari with
the variables is not particular strong in any direction (indicated by the short arrow). This suggests that some of the variance
may be explained along the third or fourth principal component etc.

4 Discussion and conclusions

The multivariate data analysis shows that host model characteristics (especially SW_CRF) are important for the modeled
205 cloudy sky contribution to RFari, but also that many factors are important. Furthermore, several other studies presented here
show that aerosol properties (in particular SSA) are important for this quantity. Locally and especially in regions with aerosols
above clouds as well as in single model studies the SSA is crucial for cloudy sky contribution to RFari. However, analyzing
multi-model simulations then additional factors are becoming important. The two AeroCom phases give cloudy sky
contribution to RFari estimates of $0.0 \pm 0.10 \text{ Wm}^{-2}$ and $0.04 \pm 0.10 \text{ Wm}^{-2}$ and the mean of two observational based methods is
210 -0.02 (range from -0.13 to 0.09 Wm^{-2}). Combining the numbers from these three studies, we find $0.01 \pm 0.1 \text{ Wm}^{-2}$ for the
cloudy sky contribution to all sky RFari. The new emission inventory from CEDS has a strong increase in BC emissions
leading to an increase in cloudy sky contribution to RFari of 0.05 Wm^{-2} from 2000 to 2014 in OsloCTM3. Using OsloCTM3
simulations to investigate the importance of using diagnostics for every radiation time step (3 hourly) shows differences up to
 0.01 W m^{-2} relative to daily mean data and up to 0.04 W m^{-2} for monthly data, but this may be model dependent (Haywood
215 and Shine, 1997).

Determining the quantity of black carbon from instrumentation such as the SP2 has provided a new set of consistent data for
assessing the performance of aerosol models (e.g. Kipling et al. (2013); Wang et al. (2014)). Knowledge of BC mass is
fundamentally insufficient for determining the ambient aerosol single scattering albedo owing to additional complexities such
as the degree of internal and external mixing. In the past, the aerosol modelling community has relied either on indirect



220 remotely sensed measurements from AERONET (e.g. Chin et al. (2009)) or on imperfect in-situ measurements of aerosol
scattering from nephelometers (e.g. Anderson et al. (2003)) and absorption from filter-based systems (e.g. Bond et al. (1999)).
Both of these systems are relatively imprecise corrections to account for scattering and absorption artifacts (e.g. Davies et al.
(2019); Massoli et al. (2009)). The single scattering albedos can be determined much more accurately using combinations of
cavity ring-down measurements of extinction (e.g. Lack et al. (2006)) and photoacoustic measurements of aerosol absorption
225 (e.g. Baynard et al. (2006)). These instruments are becoming more routine on aircraft equipped for making atmospheric
measurements that can make highly accurate assessments of the aerosol single scattering albedo at above-cloud altitudes (e.g.
Davies et al. (2019); Langridge et al. (2011)). These measurements will provide an invaluable additional source of data for
model evaluation.

Koffi et al. (2016); Koffi et al. (2012) show that global aerosol models generally tend to have an overabundance of
230 aerosols at higher altitude compared to satellite retrievals from CALIPSO and Samset et al. (2014) show that the AeroCom
models overestimate BC at mid and high tropospheric altitudes compared to aircraft measurements. Too much BC above the
clouds would overestimate the contribution of the cloudy sky to RFari. On the other hand, Peers et al. (2016) show that over
the biomass burning region in south Africa most of the AeroCom models underestimate the AAOD over the stratocumulus
layer, which would underestimate the contribution of cloudy sky to RFari.

235 In future studies of RFari, particular attention should be put on how global aerosol models simulate the location of
aerosols in relation to clouds and how aerosol optical properties change with altitude in regions with high cloud cover compared
to measurements in order to further constrain the spread in the modelled cloudy sky contribution. Nowhere is this high
sensitivity more clearly demonstrated than over the SE Atlantic where biomass burning aerosols over-lie (and sometimes
interact with) relatively bright stratocumulus clouds (e.g. Zuidema et al. (2016)). In addition to further analysis of aerosol RF
240 in cloudy sky regions, more emphasis should be devoted to quantifying the RFari in cloud free regions and its trend (Paulot
et al., 2018), where the magnitude of forcing is larger than in cloudy regions.

Acknowledgments, Samples, and Data

All AeroCom data are available at the AeroCom server (<https://aerocom.met.no/>). The OsloCTM data will be made available
through NIRD Research Data Archive. GM received funding from the Research Council of Norway through the SUPER (grant
245 250573). PS was supported by the European Research Council (ERC) project constRaining the EffeCts of Aerosols on
Precipitation (RECAP) under the European Union's Horizon 2020 research and innovation programme with grant agreement
No 724602.



References

- 250 Anderson, T. L., Masonis, S. J., Covert, D. S., Ahlquist, N. C., Howell, S. G., Clarke, A. D. and
McNaughton, C. S.: Variability of aerosol optical properties derived from in situ aircraft
measurements during ACE-Asia, *Journal of Geophysical Research: Atmospheres*, 108(D23),
2003.
- Baynard, T., Garland, R. M., Ravishankara, A. R., Tolbert, M. A. and Lovejoy, E. R.: Key factors
255 influencing the relative humidity dependence of aerosol light scattering, *Geophysical Research
Letters*, 33(6), 2006.
- Bian, H., Chin, M., Hauglustaine, D. A., Schulz, M., Myhre, G., Bauer, S. E., Lund, M. T., Karydis, V.
A., Kucsera, T. L., Pan, X., Pozzer, A., Skeie, R. B., Steenrod, S. D., Sudo, K., Tsigaridis, K.,
Tsimpidi, A. P. and Tsyro, S. G.: Investigation of global particulate nitrate from the AeroCom
phase III experiment, *Atmos. Chem. Phys.*, 17, 12911-12940, 2017.
- 260 Bond, T. C., Anderson, T. L. and Campbell, D.: Calibration and Intercomparison of Filter-Based
Measurements of Visible Light Absorption by Aerosols, *Aerosol Science and Technology*,
30(6), 582-600, 1999.
- Bond, T. C., Doherty, S. J., Fahey, D. W., Forster, P. M., Berntsen, T., DeAngelo, B. J., Flanner, M. G.,
Ghan, S., Karcher, B., Koch, D., Kinne, S., Kondo, Y., Quinn, P. K., Sarofim, M. C., Schultz,
265 M. G., Schulz, M., Venkataraman, C., Zhang, H., Zhang, S., Bellouin, N., Guttikunda, S. K.,
Hopke, P. K., Jacobson, M. Z., Kaiser, J. W., Klimont, Z., Lohmann, U., Schwarz, J. P.,
Shindell, D., Storelvmo, T., Warren, S. G. and Zender, C. S.: Bounding the role of black carbon
in the climate system: A scientific assessment, *Journal of Geophysical Research-Atmospheres*,
118(11), 5380-5552, 2013.
- 270 Boucher, O., Randall, D., Artaxo, P., Bretherton, C., Feingold, G., Forster, P., Kerminen, V.-M., Kondo,
Y., Liao, H., Lohmann, U., Rasch, P., Satheesh, S. K., Sherwood, S., Stevens, B. and Zhang, X.-
Y., Clouds and Aerosols. In: *Climate Change 2013: The Physical Science Basis. Contribution
of Working Group I to the Fifth Assessment Report of the Intergovernmental Panel on Climate
Change*. T. F. Stocker, D. Qin, G.-K. Plattner, M. Tignor, S. K. Allen et al. (Editors), Cambridge
275 University Press, Cambridge, United Kingdom and New York, NY, USA, pp. 571-657, 2013.
- Chand, D., Wood, R., Anderson, T. L., Satheesh, S. K. and Charlson, R. J.: Satellite-derived direct
radiative effect of aerosols dependent on cloud cover, *Nature Geoscience*, 2(3), 181-184, 2009.
- Chin, M., Diehl, T., Dubovik, O., Eck, T. F., Holben, B. N., Sinyuk, A. and Streets, D. G.: Light
280 absorption by pollution, dust, and biomass burning aerosols: a global model study and
evaluation with AERONET measurements, *Annales Geophysicae*, 27(9), 3439-3464, 2009.
- Davies, N. W., Fox, C., Szpek, K., Cotterell, M. I., Taylor, J. W., Allan, J. D., Williams, P. I.,
Trembath, J., Haywood, J. M. and Langridge, J. M.: Evaluating biases in filter-based aerosol
absorption measurements using photoacoustic spectroscopy, *Atmos. Meas. Tech.*, 12(6), 3417-
3434, 2019.
- 285 Forster, P., Ramaswamy, V., Artaxo, P., Berntsen, T., Betts, R., Fahey, D. W., Haywood, J., Lean, J.,
Lowe, D. C., Myhre, G., Nganga, J., Prinn, R., Raga, G., Schulz, M. and Van Dorland, R.,
Changes in Atmospheric Constituents and in Radiative Forcing. In: *Climate Change 2007: The*



- Physical Science Basis. Contribution of Working Group I to the Fourth Assessment Report of the Intergovernmental Panel on Climate Change, Cambridge University Press, Cambridge, United Kingdom and New York, NY, USA, 2007.
- 290 Haywood, J. M. and Shine, K. P.: Multi-spectral calculations of the direct radiative forcing of tropospheric sulphate and soot aerosols using a column model, *Quarterly Journal of the Royal Meteorological Society*, 123(543), 1907-1930, 1997.
- 295 Hoesly, R. M., Smith, S. J., Feng, L., Klimont, Z., Janssens-Maenhout, G., Pitkanen, T., Seibert, J. J., Vu, L., Andres, R. J., Bolt, R. M., Bond, T. C., Dawidowski, L., Kholod, N., Kurokawa, J. I., Li, M., Liu, L., Lu, Z., Moura, M. C. P., O'Rourke, P. R. and Zhang, Q.: Historical (1750–2014) anthropogenic emissions of reactive gases and aerosols from the Community Emissions Data System (CEDS), *Geosci. Model Dev.*, 11(1), 369-408, 2018.
- 300 Josse, J. and Husson, F.: Handling missing values in exploratory multivariate data analysis methods, *Journal de la Société Française de Statistique*, 153, 79–99, 2012.
- Keil, A. and Haywood, J. M.: Solar radiative forcing by biomass burning aerosol particles during SAFARI 2000: A case study based on measured aerosol and cloud properties, *Journal of Geophysical Research-Atmospheres*, 108(D13), 8467, 2003.
- Kinne, S.: Aerosol radiative effects with MACv2, *Atmos. Chem. Phys.*, 19(16), 10919-10959, 2019a.
- 305 Kinne, S.: The MACv2 aerosol climatology, *Tellus B: Chemical and Physical Meteorology*, 71(1), 1-21, 2019b.
- Kipling, Z., Stier, P., Schwarz, J. P., Perring, A. E., Spackman, J. R., Mann, G. W., Johnson, C. E. and Telford, P. J.: Constraints on aerosol processes in climate models from vertically-resolved aircraft observations of black carbon, *Atmos. Chem. Phys.*, 13(12), 5969-5986, 2013.
- 310 Koffi, B., Schulz, M., Bréon, F.-M., Dentener, F., Steensen, B. M., Griesfeller, J., Winker, D., Balkanski, Y., Bauer, S. E., Bellouin, N., Berntsen, T., Bian, H., Chin, M., Diehl, T., Easter, R., Ghan, S., Hauglustaine, D. A., Iversen, T., Kirkevåg, A., Liu, X., Lohmann, U., Myhre, G., Rasch, P., Seland, Ø., Skeie, R. B., Steenrod, S. D., Stier, P., Tackett, J., Takemura, T., Tsigaridis, K., Vuolo, M. R., Yoon, J. and Zhang, K.: Evaluation of the aerosol vertical distribution in global aerosol models through comparison against CALIOP measurements: AeroCom phase II results, *Journal of Geophysical Research: Atmospheres*, 121(12), 7254-7283, 2016.
- 315 Koffi, B., Schulz, M., Breon, F. M., Griesfeller, J., Winker, D., Balkanski, Y., Bauer, S., Berntsen, T., Chin, M. A., Collins, W. D., Dentener, F., Diehl, T., Easter, R., Ghan, S., Ginoux, P., Gong, S. L., Horowitz, L. W., Iversen, T., Kirkevåg, A., Koch, D., Krol, M., Myhre, G., Stier, P. and Takemura, T.: Application of the CALIOP layer product to evaluate the vertical distribution of aerosols estimated by global models: AeroCom phase I results, *Journal of Geophysical Research-Atmospheres*, 117, D10201, doi:10.1029/2011jd016858, 2012.
- 320 Lacagnina, C., Hasekamp, O. P. and Torres, O.: Direct radiative effect of aerosols based on PARASOL and OMI satellite observations, *Journal of Geophysical Research: Atmospheres*, 122(4), 2366-2388, 2017.
- 325



- Lack, D. A., Lovejoy, E. R., Baynard, T., Pettersson, A. and Ravishankara, A. R.: Aerosol Absorption Measurement using Photoacoustic Spectroscopy: Sensitivity, Calibration, and Uncertainty Developments, *Aerosol Science and Technology*, 40(9), 697-708, 2006.
- 330 Lamarque, J., Bond, T., Eyring, V., Granier, C., Heil, A., Klimont, Z., Lee, D., Liousse, C., Mieville, A., Owen, B., Schultz, M., Shindell, D., Smith, S., Stehfest, E., Van Aardenne, J., Cooper, O., Kainuma, M., Mahowald, N., McConnell, J., Naik, V., Riahi, K. and van Vuuren, D.: Historical (1850-2000) gridded anthropogenic and biomass burning emissions of reactive gases and aerosols: methodology and application, *Atmospheric Chemistry and Physics*, 7017-7039, 2010.
- 335 Langridge, J. M., Richardson, M. S., Lack, D., Law, D. and Murphy, D. M.: Aircraft Instrument for Comprehensive Characterization of Aerosol Optical Properties, Part I: Wavelength-Dependent Optical Extinction and Its Relative Humidity Dependence Measured Using Cavity Ringdown Spectroscopy, *Aerosol Science and Technology*, 45(11), 1305-1318, 2011.
- Lund, M. T., Myhre, G., Haslerud, A. S., Skeie, R. B., Griesfeller, J., Platt, S. M., Kumar, R., Myhre, C. L. and Schulz, M.: Concentrations and radiative forcing of anthropogenic aerosols from 1750 to 2014 simulated with the Oslo CTM3 and CEDS emission inventory, *Geosci. Model Dev.*, 11(12), 4909-4931, 2018.
- 340
- Massoli, P., Murphy, D. M., Lack, D. A., Baynard, T., Brock, C. A. and Lovejoy, E. R.: Uncertainty in Light Scattering Measurements by TSI Nephelometer: Results from Laboratory Studies and Implications for Ambient Measurements, *Aerosol Science and Technology*, 43(11), 1064-1074, 2009.
- 345
- Matus, A. V., L'Ecuyer, T. S. and Henderson, D. S.: New Estimates of Aerosol Direct Radiative Effects and Forcing From A-Train Satellite Observations, *Geophysical Research Letters*, 46(14), 8338-8346, 2019.
- 350
- Myhre, G.: Consistency between satellite-derived and modeled estimates of the direct aerosol effect, *Science*, 325(5937), 187-190, 2009.
- Myhre, G., Samset, B. H., Schulz, M., Balkanski, Y., Bauer, S., Berntsen, T. K., Bian, H., Bellouin, N., Chin, M., Diehl, T., Easter, R. C., Feichter, J., Ghan, S. J., Hauglustaine, D., Iversen, T., Kinne, S., Kirkevag, A., Lamarque, J. F., Lin, G., Liu, X., Lund, M. T., Luo, G., Ma, X., van Noije, T., Penner, J. E., Rasch, P. J., Ruiz, A., Seland, O., Skeie, R. B., Stier, P., Takemura, T., Tsigaridis, K., Wang, P., Wang, Z., Xu, L., Yu, H., Yu, F., Yoon, J. H., Zhang, K., Zhang, H. and Zhou, C.: Radiative forcing of the direct aerosol effect from AeroCom Phase II simulations, *Atmospheric Chemistry and Physics*, 13(4), 1853-1877, 2013a.
- 355
- Myhre, G., Shindell, D., Bréon, F.-M., Collins, W., Fuglestedt, J., Huang, J., Koch, D., Lamarque, J.-F., Lee, D., Mendoza, B., Nakajima, T., Robock, A., Stephens, G., Takemura, T. and Zhang, H., Anthropogenic and Natural Radiative Forcing. In: *Climate Change 2013: The Physical Science Basis. Contribution of Working Group I to the Fifth Assessment Report of the Intergovernmental Panel on Climate Change*. T. F. Stocker, D. Qin, G.-K. Plattner, M. Tignor, S. K. Allen et al. (Editors), Cambridge University Press, Cambridge, United Kingdom and New York, NY, USA, pp. 659-740, 2013b.
- 360
- 365



- Oikawa, E., Nakajima, T., Inoue, T. and Winker, D.: A study of the shortwave direct aerosol forcing using ESSP/CALIPSO observation and GCM simulation, *Journal of Geophysical Research: Atmospheres*, 118(9), 3687-3708, 2013.
- 370 Oikawa, E., Nakajima, T. and Winker, D.: An Evaluation of the Shortwave Direct Aerosol Radiative Forcing Using CALIOP and MODIS Observations, *Journal of Geophysical Research: Atmospheres*, 123(2), 1211-1233, 2018.
- Paulot, F., Paynter, D., Ginoux, P., Naik, V. and Horowitz, L. W.: Changes in the aerosol direct radiative forcing from 2001 to 2015: observational constraints and regional mechanisms, *Atmos. Chem. Phys.*, 18(17), 13265-13281, 2018.
- 375 Peers, F., Bellouin, N., Waquet, F., Ducos, F., Goloub, P., Mollard, J., Myhre, G., Skeie, R. B., Takemura, T., Tanré, D., Thieuleux, F. and Zhang, K.: Comparison of aerosol optical properties above clouds between POLDER and AeroCom models over the South East Atlantic Ocean during the fire season, *Geophysical Research Letters*, 43(8), 3991-4000, 2016.
- 380 Samset, B. H., Myhre, G., Herber, A., Kondo, Y., Li, S. M., Moteki, N., Koike, M., Oshima, N., Schwarz, J. P., Balkanski, Y., Bauer, S. E., Bellouin, N., Berntsen, T. K., Bian, H., Chin, M., Diehl, T., Easter, R. C., Ghan, S. J., Iversen, T., Kirkevåg, A., Lamarque, J. F., Lin, G., Liu, X., Penner, J. E., Schulz, M., Seland, Ø., Skeie, R. B., Stier, P., Takemura, T., Tsigaridis, K. and Zhang, K.: Modelled black carbon radiative forcing and atmospheric lifetime in AeroCom Phase II constrained by aircraft observations, *Atmos. Chem. Phys.*, 14(22), 12465-12477, 2014.
- 385 Samset, B. H., Myhre, G., Schulz, M., Balkanski, Y., Bauer, S., Berntsen, T. K., Bian, H., Bellouin, N., Diehl, T., Easter, R. C., Ghan, S. J., Iversen, T., Kinne, S., Kirkevåg, A., Lamarque, J. F., Lin, G., Liu, X., Penner, J. E., Seland, O., Skeie, R. B., Stier, P., Takemura, T., Tsigaridis, K. and Zhang, K.: Black carbon vertical profiles strongly affect its radiative forcing uncertainty, *Atmospheric Chemistry and Physics*, 13(5), 2423-2434, 2013.
- 390 Samset, B. H., Stjern, C. W., Andrews, E., Kahn, R. A., Myhre, G., Schulz, M. and Schuster, G. L.: Aerosol Absorption: Progress Towards Global and Regional Constraints, *Current Climate Change Reports*, 4(2), 65-83, 2018.
- Schulz, M., Textor, C., Kinne, S., Balkanski, Y., Bauer, S., Berntsen, T., Berglen, T., Boucher, O., Dentener, F., Guibert, S., Isaksen, I. S. A., Iversen, T., Koch, D., Kirkevåg, A., Liu, X., 395 Montanaro, V., Myhre, G., Penner, J. E., Pitari, G., Reddy, S., Seland, O., Stier, P. and Takemura, T.: Radiative forcing by aerosols as derived from the AeroCom present-day and pre-industrial simulations, *Atmospheric Chemistry and Physics*, 6, 5225-5246, 2006.
- Schutgens, N. A. J.: Site representativity of AERONET and GAW remotely sensed AOT and AAOT observations, *Atmos. Chem. Phys. Discuss.*, 2019, 1-29, 2019.
- 400 Sherwood, S. C., Bony, S., Boucher, O., Bretherton, C., Forster, P. M., Gregory, J. M. and Stevens, B.: Adjustments in the Forcing-Feedback Framework for Understanding Climate Change, *Bulletin of the American Meteorological Society*, 96(2), 217-228, 2015.
- Smith, C. J., Kramer, R. J., Myhre, G., Forster, P. M., Soden, B. J., Andrews, T., Boucher, O., Faluvegi, G., Fläschner, D., Hodnebrog, Ø., Kasoar, M., Kharin, V., Kirkevåg, A., Lamarque, J.-F., 405 Mülmenstädt, J., Olivie, D., Richardson, T., Samset, B. H., Shindell, D., Stier, P., Takemura, T.,



- Voulgarakis, A. and Watson-Parris, D.: Understanding Rapid Adjustments to Diverse Forcing Agents, *Geophysical Research Letters*, 45(21), 12,023-12,031, 2018.
- 410 Stier, P., Schutgens, N. A. J., Bellouin, N., Bian, H., Boucher, O., Chin, M., Ghan, S., Huneus, N., Kinne, S., Lin, G., Ma, X., Myhre, G., Penner, J. E., Randles, C. A., Samset, B., Schulz, M., Takemura, T., Yu, F., Yu, H. and Zhou, C.: Host model uncertainties in aerosol radiative forcing estimates: results from the AeroCom Prescribed intercomparison study, *Atmospheric Chemistry and Physics*, 13(6), 3245-3270, 2013.
- 415 Takemura, T., Nakajima, T., Dubovik, O., Holben, B. N. and Kinne, S.: Single-scattering albedo and radiative forcing of various aerosol species with a global three-dimensional model, *Journal of Climate*, 15(4), 333-352, 2002.
- 420 Tsigaridis, K., Daskalakis, N., Kanakidou, M., Adams, P. J., Artaxo, P., Bahadur, R., Balkanski, Y., Bauer, S. E., Bellouin, N., Benedetti, A., Bergman, T., Berntsen, T. K., Beukes, J. P., Bian, H., Carslaw, K. S., Chin, M., Curci, G., Diehl, T., Easter, R. C., Ghan, S. J., Gong, S. L., Hodzic, A., Hoyle, C. R., Iversen, T., Jathar, S., Jimenez, J. L., Kaiser, J. W., Kirkevåg, A., Koch, D., Kokkola, H., Lee, Y. H., Lin, G., Liu, X., Luo, G., Ma, X., Mann, G. W., Mihalopoulos, N., Morcrette, J. J., Müller, J. F., Myhre, G., Myriokefalitakis, S., Ng, N. L., O'Donnell, D., Penner, J. E., Pozzoli, L., Pringle, K. J., Russell, L. M., Schulz, M., Sciare, J., Seland, Ø., Shindell, D. T., Sillman, S., Skeie, R. B., Spracklen, D., Stavrou, T., Steenrod, S. D., Takemura, T., Tiitta, P., Tilmes, S., Tost, H., van Noije, T., van Zyl, P. G., von Salzen, K., Yu, F., Wang, Z., Wang, Z., Zaveri, R. A., Zhang, H., Zhang, K., Zhang, Q. and Zhang, X.: The AeroCom evaluation and intercomparison of organic aerosol in global models, *Atmos. Chem. Phys.*, 14(19), 10845-10895, 2014.
- 425 Wang, Q. Q., Jacob, D. J., Spackman, J. R., Perring, A. E., Schwarz, J. P., Moteki, N., Marais, E. A., Ge, C., Wang, J. and Barrett, S. R. H.: Global budget and radiative forcing of black carbon aerosol: Constraints from pole-to-pole (HIPPO) observations across the Pacific, *Journal of Geophysical Research-Atmospheres*, 119(1), 195-206, 2014.
- 430 Wang, R., Andrews, E., Balkanski, Y., Boucher, O., Myhre, G., Samset, B. H., Schulz, M., Schuster, G. L., Valari, M. and Tao, S.: Spatial Representativeness Error in the Ground-Level Observation Networks for Black Carbon Radiation Absorption, *Geophysical Research Letters*, 45(4), 2106-2114, 2018.
- 435 Zhang, Z., Meyer, K., Yu, H., Platnick, S., Colarco, P., Liu, Z. and Oreopoulos, L.: Shortwave direct radiative effects of above-cloud aerosols over global oceans derived from 8 years of CALIOP and MODIS observations, *Atmos. Chem. Phys.*, 16(5), 2877-2900, 2016.
- 440 Zuidema, P., Redemann, J., Haywood, J., Wood, R., Piketh, S., Hipondoka, M. and Formenti, P.: Smoke and Clouds above the Southeast Atlantic: Upcoming Field Campaigns Probe Absorbing Aerosol's Impact on Climate, *Bulletin of the American Meteorological Society*, 97(7), 1131-1135, 2016.



445 **Tables**

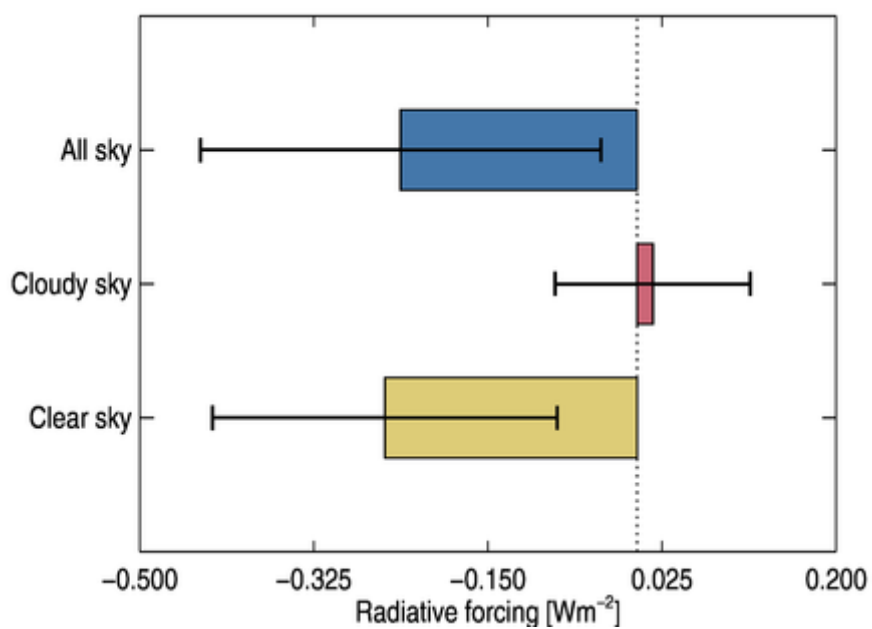
450 **Table 1. Diagnostics from AeroCom Phase 2 (Myhre et al., 2013a; Samset et al., 2013; Stier et al., 2013) used in multivariate data analysis to investigate factors influencing the contribution of cloudy sky to RFari. The variable “Cloudy” is the contribution of cloudy sky to RFari (second term on the right-hand side of equation 1). FIX2scat and FIX3abs are the contributions from cloudy sky to RFari in two highly idealized aerosol radiative properties experiments in Stier et al. (2013), where FIX2scat is a purely scattering aerosol case and FIX3abs is an absorbing aerosol case. The other variables, from AeroCom phase II model simulations, are total short-wave cloud radiative effect (SW_CRF), cloud fraction (CLD_FR), weighed cloud height (CL_ALT), weighted anthropogenic aerosol height (AER_ALT), single scattering albedo (SSA) of anthropogenic aerosols and fraction of anthropogenic BC mass above 5 km (BC_mass_5km). The variables Cloudy, FIX2, FIX3 and SW_CRF are given in Wm⁻², CLD_FR and BC mass>5km in percent, with SSA unitless. AER_ALT and CL_ALT are given in hPa where the pressure levels are weighted by aerosol extinction and cloud fractions, respectively.**

Models	Cloudy	Host model dependences					Aerosol properties		
		FIX2scat	FIX3abs	SW CRF	CLD FR	CL ALT	AER ALT	SSA	BC mass >5km
	W m ⁻²	W m ⁻²	W m ⁻²	W m ⁻²	%	hPa	hPa	1	%
CAM5	0.121	-1.8	1.8	-48.4	64	592	908	0.901	18.1
GOCART	-0.114	-1.6	1.2	-21.8	58	520	867	0.937	27.1
HadGEM2	0.0554	-1.1	1.5	-53.1	55	638	921	0.947	33.6
IMPACT	0.114	-1.5	2.1	-68.6	66	554	850	0.973	5.8
LMDZ-INCA	0.0756	-0.8	2.5	-53.1	47	585	NA	0.968	28.9
ECHAM-HAM	-0.0242	-1.7	1.1	NA	63	NA	NA	0.936	10.8
OsloCTM2	0.0934	-1.4	1.4	-49.3	62	616	885	0.939	30.1
SPRINTARS	0.155	-1.5	1.7	-47.4	60	525	913	0.958	30.3

460

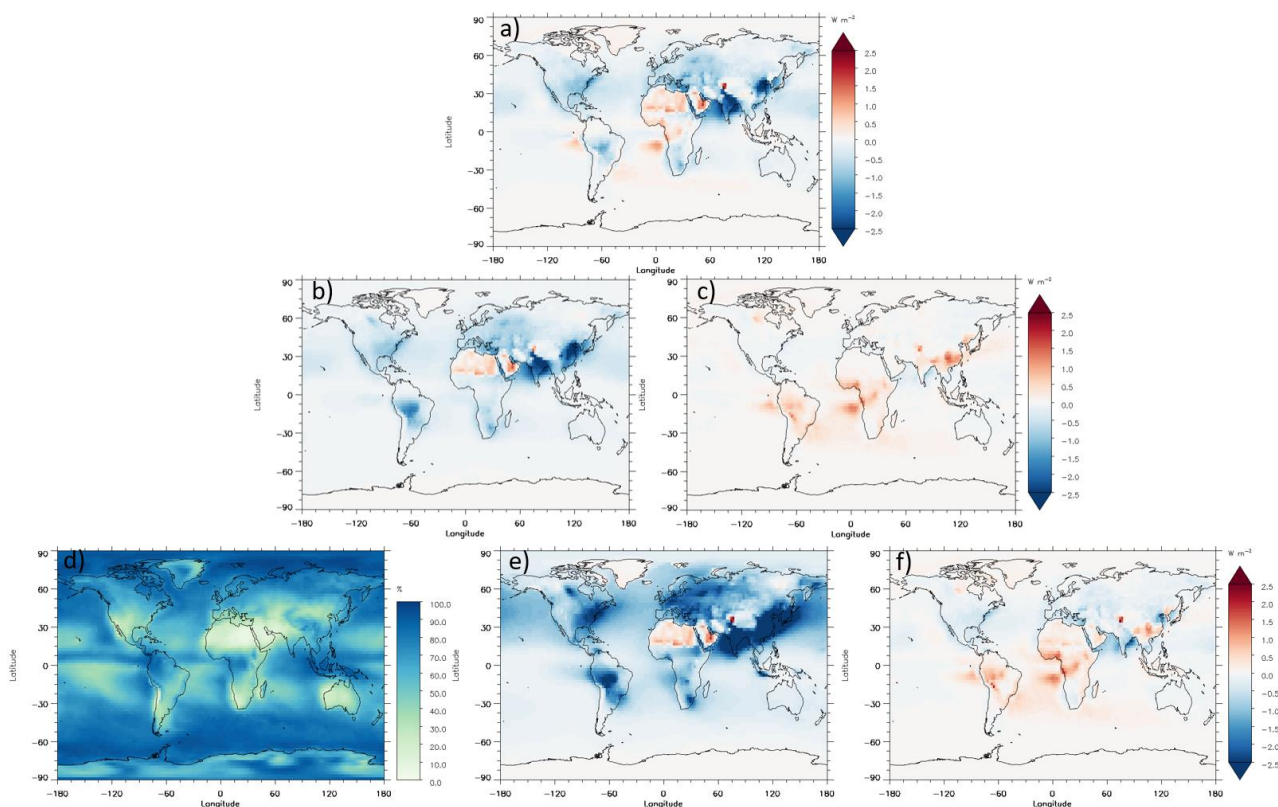


Figures



465

Figure 1: All sky RFari, the contribution from cloud sky and clear sky to RFari (second and first term on the right hand of equation 1, respectively) from AeroCom Phase II simulations (Myhre et al., 2013a).



470

Figure 2. Annual mean all sky R_{Far} and various terms from clear and cloudy skies simulated with OsloCTM3 (Lund et al., 2018). The panel in the top row is the all sky R_{Far} a), the second row shows the contributions from clear and cloudy sky (first b) and second term c) on right hand side on equation 1, respectively). The third row shows cloud fraction d), $R_{Far,clear}$ e) and $R_{Far,cloud}$, f) respectively (see equation 1). Panel d) on cloud fraction is showed in percent and the other panels in $W m^{-2}$.

475

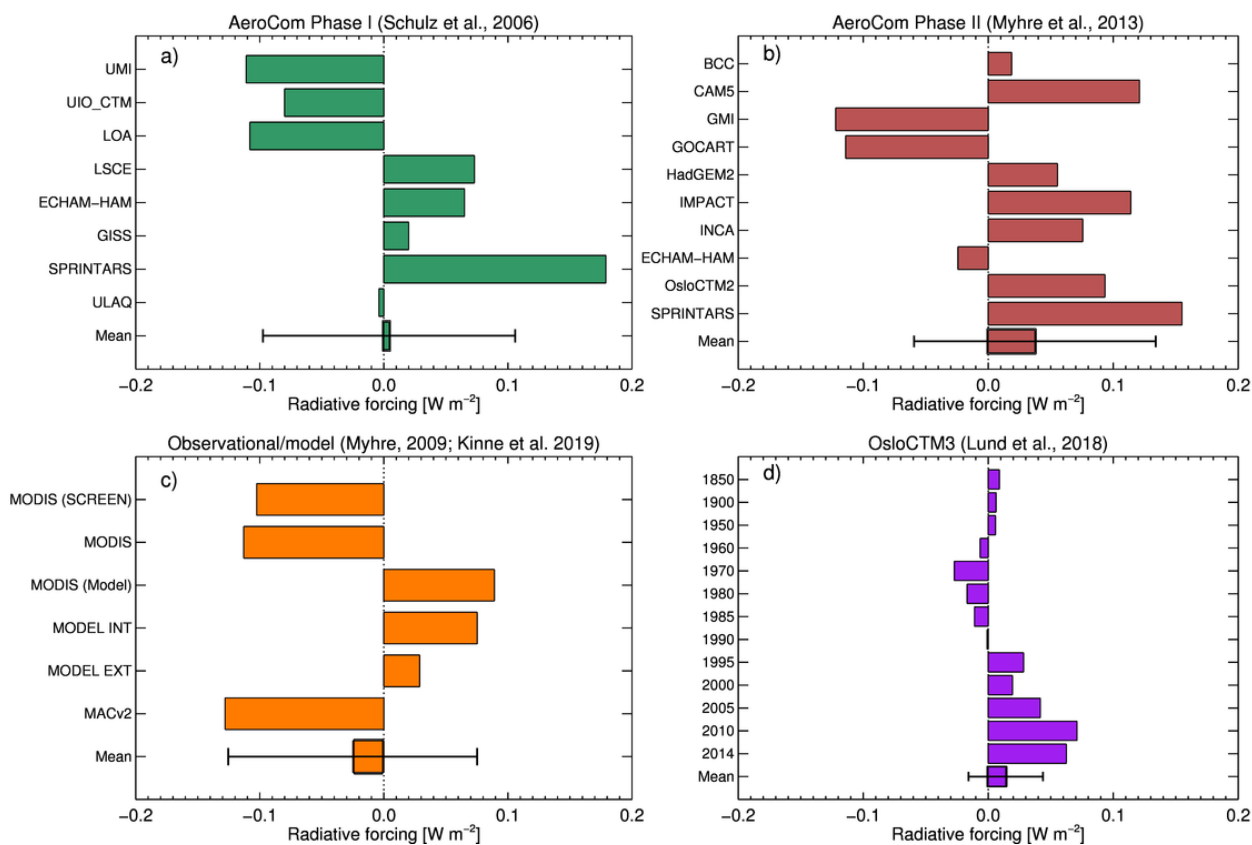
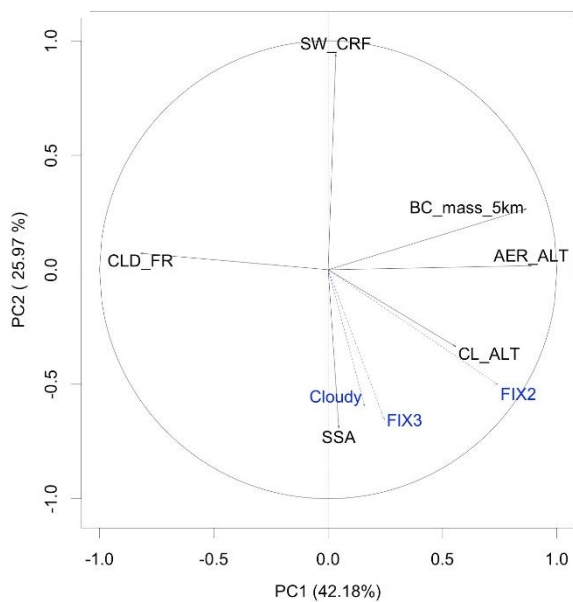


Figure 3. The contribution of cloudy sky to RFari from AeroCom Phase I (Schulz et al., 2006) (a), AeroCom Phase II (Myhre et al., 2013a) (b), combination of observational based and model simulation (Kinne, 2019a; Myhre, 2009), where mean and standard deviation are based on all methods used in the panel (c), and time evolution from OsloCTM3 (Lund et al., 2018) (d). The multi-model mean is shown by the bars and the one standard uncertainty range of the models is given by whiskers.

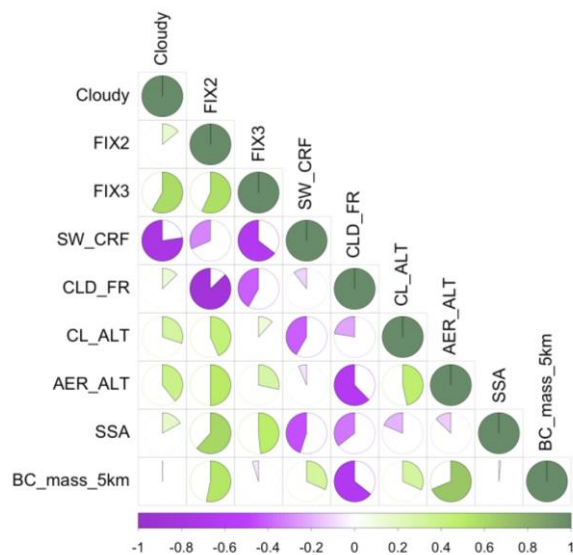
480



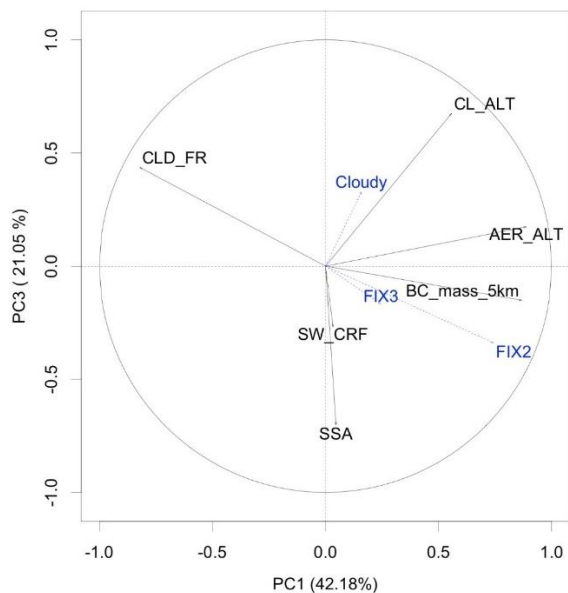
(a) PCA biplot of variables



(b) Correlogram



(c) PCA biplot of variables





485 **Figure 4. Multivariate data analysis of eight AeroCom Phase II models (Myhre et al., 2013a) using diagnostics shown in Table S1. Principal Component Analysis biplot of the variables (a). The length of the arrows indicates the strength of the correlation each variable has in relation to PC1 and PC2, representing 42.2% and 26.0% of the variance respectively. Variables clustered together indicate positive correlation with each other. Variable opposing each other indicate negative correlation. Cloudy, FIX3 and FIX2 (in blue) are added as supplementary variables, and do not influence the projection of the other variables. FIX2 and FIX3 have fixed SSA globally and for all models, where the former experiment has pure scattering aerosol and FIX3 has relatively low SSA (and thus high aerosol absorption). In (b), the correlogram shows the one to one linear regression correlation each variable has to each other. The correlation coefficients (r) are presented on a color scale from -1 (purple) to 0 (white) to +1 (green). The strength of the correlation is additionally presented as pie charts filling clockwise in green for positive correlations between two variables, and counter clockwise in purple for negative correlation, where they can range from empty and full pie charts, indicating an absolute correlation respectively from 0 to 1. Panel (c) is same as for (a), but for PC1 and PC3.**

490

495